Room temperature preparation of *c* axis oriented ZnO films on Si(100), SiO_2, and ZnO substrates by rf magnetron sputtering

N. H. Kim and H. W. Kim

Growth of ZnO thin films with c axis (002) orientation has been demonstrated at room temperature on Si(100), SiO_2, and amorphous ZnO substrates by the rf magnetron sputtering method. The structural properties of the ZnO thin films were investigated with varying rf power. X-ray diffraction analysis revealed that increasing rf power helped to increase the c axis lattice constant and grain size, regardless of substrate material. Scanning electron microscopy indicated that the structural morphology of the ZnO films was not dependent on the substrate material. BCT/613

Keywords: Amorphous ZnO, Magnetron sputtering, Thin films, Zinc oxide ceramic.

The authors are in the School of Materials Science and Engineering, Inha University, Incheon 402–751, Republic of Korea (hwkim@inha.ac.kr). *Manuscript received 2 June 2003; accepted 10 October 2003.*

INTRODUCTION

II–VI semiconductors are attractive for their potential in acoustic, electronic, and optical applications such as surface acoustic wave, acousto-optic, piezo-optic, piezoelectric, and photoelectric devices, and in particular in voltage photophosphorescent devices.[1] Zinc oxide ceramic ZnO, a direct bandgap II–VI semiconductor, is a novel photonic material. Unique properties of ZnO are a direct bandgap of 3·37 eV at room temperature, large bond strength with large exciton binding energy ($E_b = 60$ meV), and a high melting temperature of 2248 K. ZnO therefore has potential for use in optical applications such as ultraviolet lasers, blue light emitting diodes, and phosphorescent displays.

Self-textured ZnO films can be synthesised on any semiconductor substrate.[2–5] Various techniques being used to grow ZnO films include sputtering,[6–8] sol–gel processing,[9,10] spray pyrolysis,[11,12] pulsed laser deposition,[13–16] metal–organic chemical vapour deposition (MOCVD),[17,18] and molecular beam epitaxy (MBE).[19,20] Most of the literature on the subject of thin film ZnO has described deposition temperatures in the range 200–500°C. The growth of ZnO thin films at very low temperatures, such as room temperature, is very important not only to minimise the thermal budget in the fabrication process and to reduce dopant diffusion and interface broadening, but also to reduce unwanted thermal stress. However, films deposited at temperatures lower than 200°C have shown little if any crystallographic structure,[21] and a study on the improvement of the structural qualities of ZnO thin films is necessary. Although some researchers have grown ZnO films at very low temperatures such as room temperature,[22–25] the effects of substrate material on the structural characteristics of ZnO thin films have not been sufficiently investigated.

High quality ZnO films deposited on Si substrates pave the way for integration of devices with advanced Si integrated circuit technology. Also, SiO_2 substrates have obvious technological advantages and potential applications.[26] Although some researchers have reported on the possibility of homoepitaxial ZnO growth,[27,28] reports on the effects of amorphous ZnO substrates are rare.

In the present work, ZnO thin films were deposited on various substrates such as Si(001), SiO_2, and amorphous ZnO at room temperature using an rf magnetron sputtering technique, and the effects of rf power on the structural properties of the films were studied. Since the growth rate increases with increasing rf power, in order to investigate the genuine effect of rf power the thickness of the sputtered ZnO layer was fixed. The structural properties of the ZnO films were studied using X-ray diffraction and scanning electron microscopy.

EXPERIMENTAL PROCEDURES

A schematic description of the rf sputtering system is provided elsewhere.[29] ZnO films were deposited by an rf magnetron sputtering system using a ZnO (99·99% purity) target with diameter and thickness of 75 and 6 mm respectively. Sputtering was carried out in a 30 smL Ar (99·99% purity) gas atmosphere at 80–250 W rf power. The magnetron was capacitively powered at 13·56 MHz rf. ZnO thin films were sputtered on Si(100), SiO_2, and amorphous ZnO substrates.

The Si substrate was *p* type silicon with (100) orientation and 1–30 Ω cm resistivity. The Si substrate was cleaned in acetone for 10 min, HF (20:1) for 10 s, and then rinsed in deionised water for 1 min before loading into the sputtering system. The SiO_2 substrate was produced by thermally growing a 60 nm SiO_2 layer on the Si(100) substrate. The ZnO substrate was subsequently made by depositing a 100 nm ZnO film on the SiO_2 substrate by MOCVD, using diethyl zinc $Zn(C_2H_5)_2$ (99·9999% purity) and O_2 gas (99·999% purity) as source gases at a temperature of 25°C. The MOCVD system used has been described elsewhere.[30] The SEM image and the XRD diffraction pattern of the ZnO thin film used as substrate indicate that an amorphous ZnO film was formed (not shown). Before loading into the reactor, the SiO_2 and ZnO substrates were cleaned in acetone for 10 min and then rinsed in deionised water for 1 min.

The chamber pressure was reduced to 6×10^{-6} torr (8×10^{-6} mbar) using a turbomolecular pump before introducing the Ar sputtering gas. The substrate temperature was monitored using a thermocouple attached near the substrate. The ZnO film was grown at room temperature at a pressure of $5{\cdot}0 \times 10^{-2}$ torr. The physical structure of the films (crystalline structure and microstructure) was analysed by XRD using Cu $K_{\alpha 1}$ radiation ($\lambda = 0{\cdot}154056$ nm) and SEM (Hitachi S-4200).

RESULTS AND DISCUSSION

In order to reveal the effect of rf power, excluding the film thickness effect, film thickness was set at about 400–600 nm. The dependence of film growth rate on rf power is shown

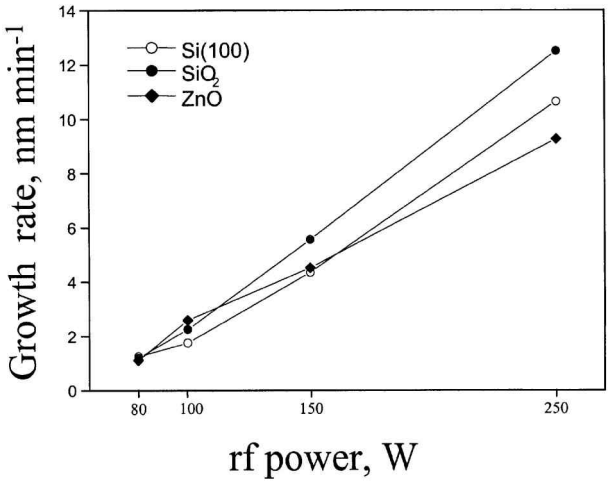

1 Dependence of ZnO film growth rate on rf power and substrate material

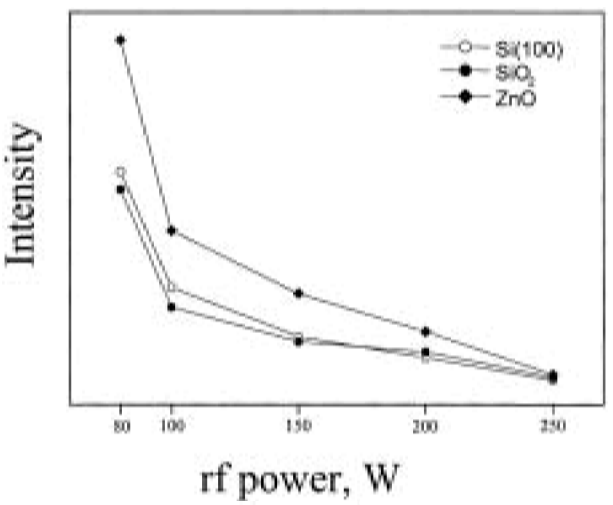

2 Relative intensity of ZnO films deposited on given substrates as function of rf power

in Fig. 1, indicating that the growth rate is almost linearly proportional to rf power, regardless of substrate material. For the whole range of deposition parameters used in this experiment, the XRD of all ZnO thin films showed *c* axis orientation, exhibiting only the (002) and (004) diffraction peaks (not shown). The θ–2θ scan data of ZnO films exhibit

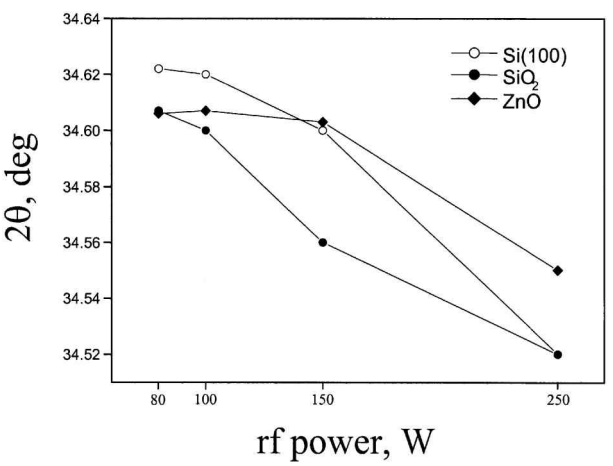

3 XRD peak angles of ZnO films deposited on given substrates as function of rf power

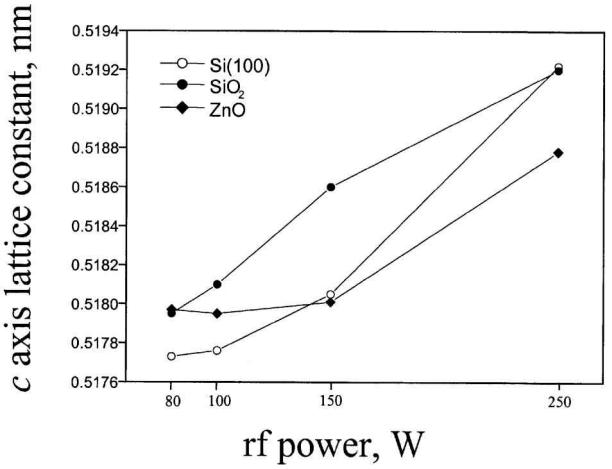

4 Variation of *c* axis lattice constant of ZnO films deposited on given substrates as function of rf power

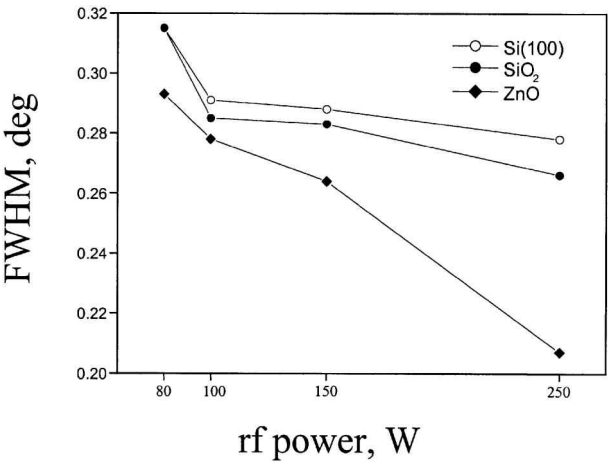

5 Full width at half maximum of ZnO films deposited on given substrates as function of rf power

strong 2θ peaks at 34·53°, corresponding to the (002) peaks of ZnO. Since the *c* axis (002) diffraction peaks were distinguishable in the ZnO films, it is surmised that *c* axis oriented ZnO film is obtained regardless of substrate material. Figure 2 shows the relative intensity of ZnO films deposited on various substrates with (002) orientation, as

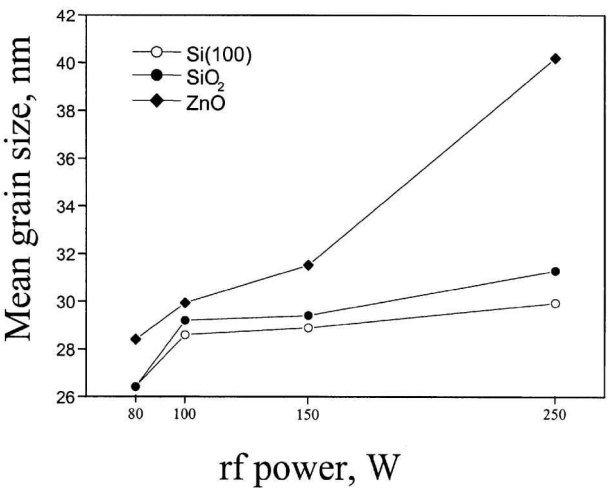

6 Mean grain size of ZnO films deposited on given substrates as function of rf power: grain size calculated using Scherrer formula

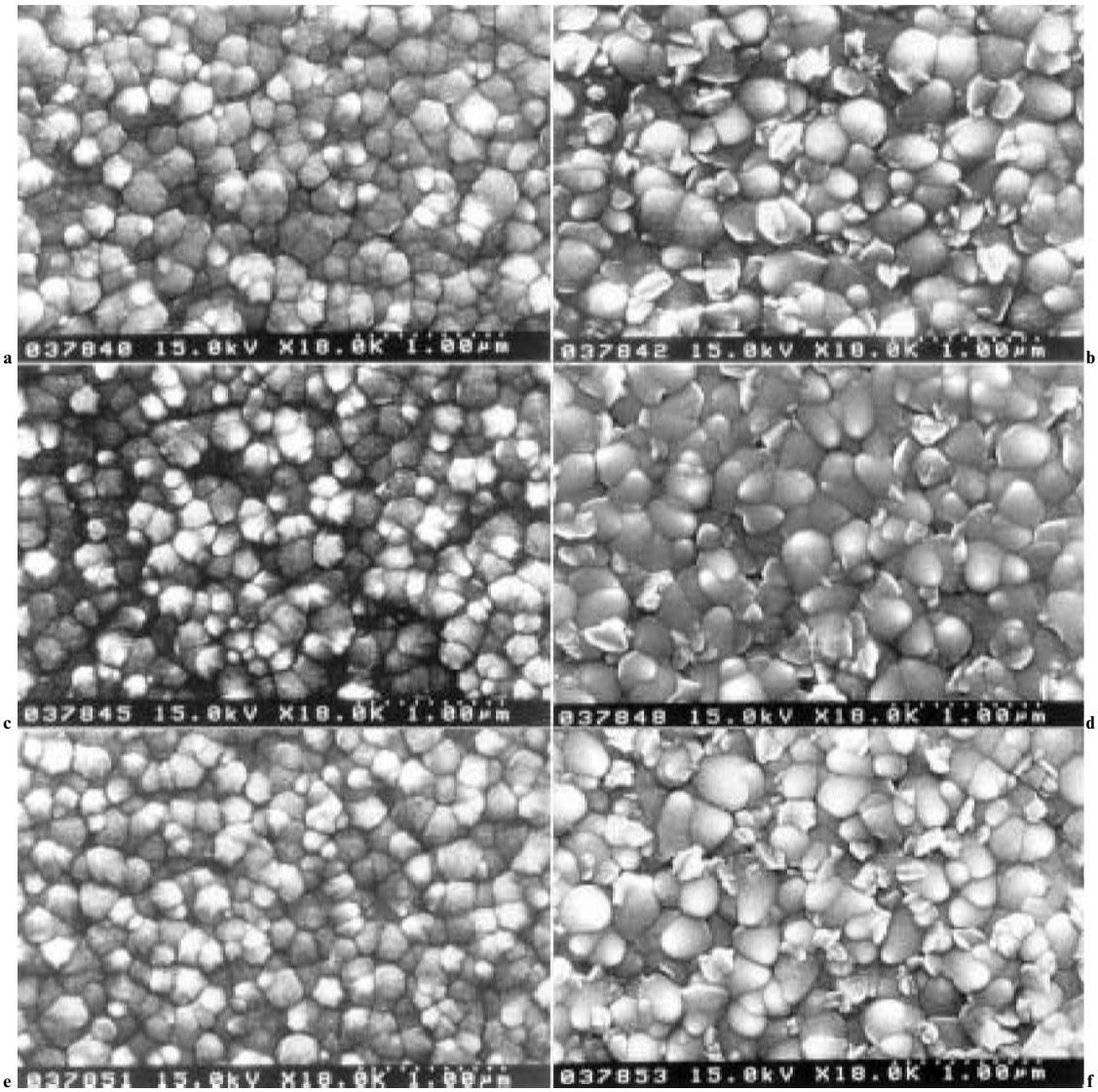

7 Plain view SEM images of ZnO thin films deposited on *a*,*b* Si(100), *c*,*d* SiO_2, *e*,*f* amorphous ZnO substrates at room temperature, at rf powers of 100 W (*a*,*c*,*e*) and 250 W (*b*,*d*,*f*)

a function of rf power ranging from 80 to 250 W, indicating that relative intensity increases with decreasing rf power.

Figure 3 shows the XRD peak angles of ZnO film deposited on various substrates with the (002) orientation, as a function of rf power ranging from 80 to 250 W, revealing that the (002) XRD peak angles of ZnO films decrease with increasing rf power. The *c* axis lattice constant is calculated using the Bragg equation and shown in Fig. 4, revealing a constant increase with increasing rf power. Since the XRD angle (2θ) and the *c* axis lattice parameter of the bulk ZnO are 34·44° and 0·5204 nm respectively, compressive stress in the *c* axis direction exists within the ZnO thin film deposited at room temperature. It is not clear why reducing rf power increases the compressive stress in the *c* axis direction and thus reduces the *c* axis lattice constant in these experiments. Further systematic study is under way to explain the observed phenomena.

Figure 5 shows the full width at half maximum (FWHM) of ZnO films deposited on various substrates with (002) orientation, as a function of rf power ranging from 80 to 250 W. The values of FWHM for the (002) diffraction peaks of ZnO films deposited on amorphous ZnO layers at 80, 100, 150, and 250 W are 0·293, 0·278, 0·264, and 0·207° respectively. FWHM decreases with increasing rf power, regardless of substrate material. To evaluate the mean grain size *D* of films on the basis of the XRD results, the Scherrer formula $D = 0{\cdot}9\lambda/B\cos\theta$ was applied,[31] where λ, B, θ are X-ray wavelength (1·54056 Å), the FWHM of the ZnO (002) diffraction peak, and the Bragg diffraction angle, respectively. By this calculation, the mean grain sizes of the ZnO films deposited on the amorphous ZnO layers are found to be 28·4, 29·0, 31·5, and 40·2 nm at 80, 100, 150, and 250 W respectively. The calculated mean grain sizes of the ZnO films are plotted in Fig. 6, revealing that the mean grain size increases with increasing rf power, regardless of substrate material. Thus it is surmised that the increase in *c* axis lattice constant with increasing rf power is due to increasing grain size in the *c* axis direction.

Figure 7 shows plain view SEM images of ZnO thin films deposited at room temperature, at rf powers of 100 and 250 W. The images indicate a slight increase in the grain size on top of the ZnO film with increasing rf power from 100 to 250 W. Since the substrate temperature during sputtering at rf powers of 80, 100, 150, and 250 W is calculated to be 33, 40, 55, and 76°C, respectively, it is surmised that the temperature elevation at higher rf power helps to produce the slightly larger grain structure. It is noteworthy that the grain size on top of the ZnO film is not much dependent on substrate material. Figure 8 shows cross-sectional SEM images of ZnO films deposited at room temperature at an rf power of 150 W, revealing that the lower part of the films consists of cloudy small grained

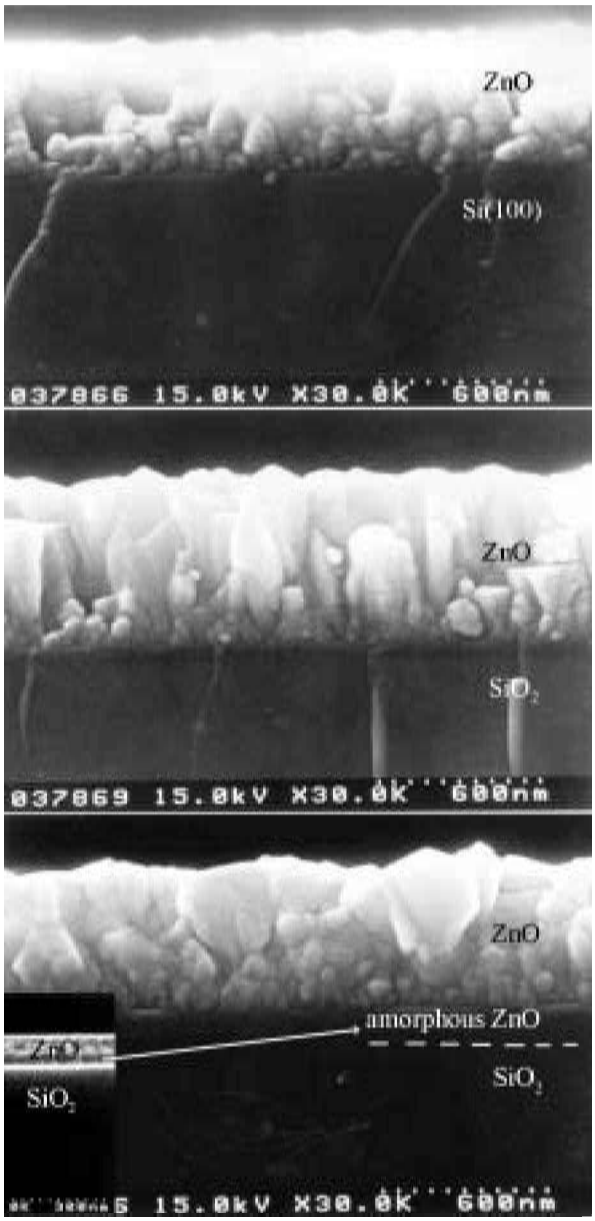

8 Cross-sectional SEM images of ZnO thin films deposited on *a* Si(100), *b* SiO_2, *c* amorphous ZnO substrates at room temperature, at rf power of 150 W: inset shows amorphous ZnO layer before ZnO deposition

structures. On the other hand, the top part of the films is made up of columnar large grained structures. The grain morphology of the ZnO films is not dependent on substrate material. It is surmised that the ZnO films deposited at room temperature have smaller grains initially, and as growth proceeds the cloudy small grained structures change into larger grained columnar structures, regardless of substrate material.

CONCLUSIONS

ZnO thin films have been grown on Si(100), SiO_2, and amorphous ZnO substrates at room temperature. XRD of all films showed *c* axis orientation, regardless of rf power and substrate material. The XRD (002) peak angle decreases and thus the *c* axis lattice parameter increases with increasing rf power. The FWHM and relative intensity of the (002) diffraction peak decrease with increasing rf power. SEM images indicate that even though the grain size of ZnO film increases slightly with increasing rf power, grain size and grain morphology do not depend on substrate material. It is believed that this approach to investigating the very low temperature growth of ZnO films on various substrate materials is a step towards the efficient production of ZnO devices.

ACKNOWLEDGEMENT

This work was supported by grant R05-2001-000-00843-0 from the Basic Research Program of the Korea Science & Engineering Foundation.

REFERENCES

1. R. VISPUTE, V. TALYANSKY, R. P. SHARMA, S. CHOOPAN, M. DOWNES, T. VENKATESAN, Y. X. LI, L. G. SALAMANCA-RIBA, A. A. ILIAD, K. A. JONES and J. MCGARRITY: *Appl. Surf. Sci.*, 1998, **127–129**, 431–439.
2. B. J. JIN, S. IM and S. Y. LEE: *Thin Solid Films*, 2000, **366**, 107–110.
3. L. N. DINH, M. A. SCHILDBACH, M. BALLOCH and W. MCLEAN: *J. Appl. Phys.*, 1999, **86**, 1149–1152.
4. Y. R. RYU, S. ZHU, J. M. WROBEL, H. M. JEONG, P. F. MICELI and H. W. WHITE: *J. Cryst. Growth*, 2000, **216**, 326–329.
5. Y. R. RYU, S. ZHU, D. C. LOOK, J. M. WROBEL, H. M. JEONG and H. W. WHITE: *J. Cryst. Growth*, 2000, **216**, 330–334.
6. R. ONDO-NDONG, F. PASCAL-DELANNOY, A. BOYER, A. GIANI and A. FOUCARAN: *Mater. Sci. Eng. B*, 2003, **97**, 68–73.
7. S. MANIV and A. ZANGVIL: *J. Appl. Phys.*, 1978, **49**, 2787–2792.
8. K. B. SUNDARAM and A. KHAN: *Thin Solid Films*, 1997, **295**, 87–91.
9. J.-H. LEE, K.-H. KO and B.-O. PARK: *J. Cryst. Growth*, 2003, **247**, 119–125.
10. M. N. KAMALASANAN and S. CHANDRA: *Thin Solid Films*, 1996, **288**, 112–115.
11. R. AYOUCHI, F. MARTIN, D. LEINEN and J. R. RAMOS-BARRADO: *J. Cryst. Growth*, 2003, **247**, 497–504.
12. B. J. LOKHANDE, P. S. PATIL and M. D. UPLANE: *Mater. Lett.*, 2002, **57**, 573–579.
13. J. N. ZENG, J. K. LOW, Z. M. REN, T. LIEW and Y. F. LU: *Appl. Surf. Sci.*, 2002, **197**, 362–367.
14. H. KIM, J. S. HORWITZ, S. B. QADRI and D. B. CHRISEY: *Thin Solid Films*, 2002, **420**, 107–111.
15. S. IM, B. J. JIN and S. YI: *J. Appl. Phys.*, 2000, **87**, 4558–4561.
16. S. AMIRHAGHI, V. CRACIUN, D. CRACIUN, J. ELDERS and I. W. BOYD: *Microelectron. Eng.*, 1994, **25**, 321–326.
17. G. DU, J. WANG, X. WANG, X. JIANG, S. YANG, Y. MA, W. YAN, D. GAO, X. LIU, H. CAO, J. XU and R. P. H. CHANG: *J. Cryst. Growth*, 2003, **243**, 439–443.
18. W. I. PARK and G. C. YI: *J. Electron. Mater.*, 2001, **30**, L32.
19. K. IWATA, P. FONS, S. NIKI, A. YAMADA, K. MATSUBARA, K. NAKAHARA, T. TANABE and H. TAKASU: *J. Cryst. Growth*, 2000, **214/215**, 50–54.
20. H. J. KO, Y. F. CHEN, Z. ZHU, T. YAO, I. KOBAYASHI and H. UCHIKI: *Appl. Phys. Lett.*, 2000, **76**, 1905–1907.
21. H. K. KIM, W. KLEEMEIER, Y. LI and D. W. LANGER: *J. Vac. Sci. Technol. B*, 1994, **12**, 1328–1332.
22. A. BARKER, S. CROWTHER and D. REES: *Sens. Actuators A*, 1997, **58**, 229–235.
23. Y. NAKATA, T. OKADA and M. MAEDA: *Appl. Surf. Sci.*, 2002, **197/198**, 368–370.
24. Y. L. LIU, Y. C. LIU, Y. X. LIU, D. Z. SHEN, Y. M. LU, J. Y. ZHANG and X. W. FAN: *Physica B*, 2002, **322**, 31–36.
25. K. RAMAMOORTHY, C. SANJEEVIRAJA, M. JAYACHANDRAN, K. SANKARANARAYANAN, P. BHATTACHARYA and L. M. KUKREJA: *J. Cryst. Growth*, 2001, **226**, 281–286.
26. W. S. HU, Z. G. LIU, J. SUN, X. L. GUO, Z. J. YANG, L. J. SHI and D. FENG: *Mater. Sci. Eng. B*, 1996, **40**, 165–169.
27. S. ZHU, C.-H. SU, S. L. LEHOCZKY, M. T. HARRIS, M. J. CALLAHAN, P. MCCARTY and M. A. GEORGE: *J. Cryst. Growth*, 2000, **219**, 361–367.
28. H. WENISCH, V. KIRCHNER, S. K. HONG, Y. F. CHEN, H. J. KO and T. YAO: *J. Cryst. Growth*, 2001, **227/228**, 944–949.
29. K.-S. KIM, H. W. KIM and N. H. KIM: *Physica B*, 2003, **334**, 343–346.
30. K.-S. KIM, H. W. KIM and C. M. LEE: *Mater. Sci. Eng. B*, 2003, **98**, 135–139.
31. B. D. CULLITY: 'Elements of X-ray diffraction', 102; 1967, London, Addison-Wesley.